J Radioanal Nucl Chem (2012) 292:837–852
DOI 10.1007/s10967-011-1527-7

Sorptive removal of cobalt, strontium and cesium onto manganese and iron oxide-coated montmorillonite from groundwater

Younjin Park · Won Sik Shin · Sang-June Choi

Received: 17 October 2011 / Published online: 19 November 2011

Abstract Applicability of montmorillonite, manganese oxide-coated montmorillonite (MOCM) and iron oxide-coated montmorillonite (IOCM) as backfill materials in permeable reactive barrier (PRB) to remediate contaminated groundwater was investigated. Single- and bi-solute competitive sorptions of Co, Sr and Cs were conducted. The Freundlich, Langmuir and Dubinin-Radushkevich models fitted the single-solute sorption data well ($R^2 > 0.95$). Maximum sorption capacities (q_{mL}) of Co and Sr predicted by the Langmuir model were in the order of MOCM (0.37 mmol/g for Co and 0.28 mmol/g for Sr) > montmorillonite (0.27 mmol/g for Co and 0.19 mmol/g for Sr) ≈ IOCM (0.23 mmol/g for Co and 0.21 mmol/g for Sr), while those of Cs were in the order of montmorillonite (1.11 mmol/g) > MOCM (0.68 mmol/g) > IOCM (0.62 mmol/g). In the bi-solute sorptions, the sorbed amount of one solute decreased due to the presence of the other competing metal ion. Langmuir model parameters for single-solute (q_{mL} and b_L) and bi-solute (q^*_{mL} and b^*_L) sorptions were compared to analyze the effect of competition between the metal ions. The competitive Langmuir ($R^2 > 0.81$) and P-factor ($R^2 > 0.82$) models predicted the bi-solute competitive sorption data well but not the SRS model ($0.003 < R^2 < 0.97$).

Keywords Groundwater · Iron oxide-coated montmorillonite · Manganese oxide-coated montmorillonite · Montmorillonite · Permeable reactive barrier (PRB)

Y. Park · W. S. Shin (✉) · S.-J. Choi
Department of Environmental Engineering, Kyungpook National University, 1370 Sankyuk-Dong, Buk-Gu, Daegu 702-701, Republic of Korea
e-mail: wshin@mail.knu.ac.kr

List of symbols

b_L	Langmuir model constant (L/mmol)
$b_{L,i}$	Langmuir model constant of a solute i in single-solute sorption (L/mmol)
$b^*_{L,i}$	Langmuir model constant of a solute i in bi-solute competitive sorption (L/mmol)
C	Aqueous-phase equilibrium concentration (mmol/L)
C_0	Initial concentration (mmol/L) of metal in aqueous solution
$C_{m,i}$	Aqueous-phase equilibrium concentration (mmol/L) of a solute i in bi-solute competitive sorption
CLM	Competitive Langmuir model
E	Mean free energy (kJ/mol) in Dubinin-Radushkevich model
K_F	Freundlich sorption coefficient $[(\text{mmol/g})/(\text{mmol/L})^{N_F}]$.
$K_{F,i}$	Freundlich sorption parameters obtained from a single-solute system $[(\text{mmol/g})/(\text{mmol/L})^{N_F}]$
N_d	The number of data points
N_F	Exponent in Freundlich model
$N_{F,i}$	Exponent in Freundlich model obtained from a single-solute system
P	The number of parameters
P_i	P-factor model parameter
q	Solid-phase equilibrium concentration (mmol/g)
$q_{i,exp}$	Solid-phase equilibrium concentration of the experimental data (mmol/g)
$q_{i,pred}$	Solid-phase equilibrium concentration of theoretically predicted points (mmol/g)
$q_{m,i}$	Solid-phase equilibrium concentration of a solute i in bi-solute competitive sorption (mmol/g)
q_{mD}	Maximum sorption capacity of Dubinin-Radushkevich model (mmol/g)
q_{mL}	Maximum sorption capacity of Langmuir model (mmol/g)

$q_{mL,i}$ Maximum sorption capacity of solute i in single-solute sorption predicted by Langmuir model (mmol/g)
$q^*_{mL,i}$ Maximum sorption capacity of solute i in bi-solute competitive sorption predicted by Langmuir model (mmol/g)
R Gas constant, 8.314 (J/mol/K)
R^2 Coefficient of determination
R_L Separation factor
RMSE Root mean square error
rss Residual sum of squares
SSE Sum of squared errors
T Absolute temperature (K)

Greek letters

α SRS model coefficient
$\alpha_{i,j}$ Dimensionless competition coefficient for the sorption of solute i in the presence of solute j predicted by SRS model
β Dubinin-Radushkevich model parameter (mol^2/J^2)
ε Polanyi potential (J/mol)

Introduction

Groundwater contamination by radionuclides results from many sources such as dismantlement of medical instruments containing radioisotopes, radioactive waste produced from nuclear power plants and nuclear fission products routinely or accidentally released. Several accidental groundwater contamination; Kyshtym, Three-mile Island, and Chernobyl accident with ^{137}Cs and ^{90}Sr were reported [1–3]. Recently, Fukushima (Tohoku region, the pacific coast of northeastern, Japan) nuclear releases occurred after a 9.0 magnitude earthquake and tsunami on March 11, 2011 [4]. Especially, in Chernobyl accident, five million people in the areas were exposed to the hazard levels of radioactive cesium deposition more than 37 kBq/m^2 and among them about 270,000 people continue to live in the areas classified as strictly controlled zones (SCZs), where radioactive cesium contamination exceeded 555 kBq/m^2. A great increase in the incidence of thyroid cancer, cataracts and cardiovascular diseases has occurred among the people [2, 5]. Not only historical nuclear accident but also the release of radioactivity from natural sources can create environmental problems. For example, uranium and radon in granitic zones emitted radioactivity to groundwater systems and the frequency of their emission has increased in Korea [6]. Therefore, it is highly necessary to protect groundwater and soil system from these radioactive metals.

One of the current methods available for the remediation of radionuclide-polluted groundwater is permeable reactive barrier (PRB). A PRB is placed underground in a natural aquifer and intercepts the pollution plume transported within the aquifer. In PRB technology, multiple mechanisms such as sorption, ion-exchange, oxidation–reduction and precipitation are involved in the removal of target metals. PRB technology has recently considered as an effective and economically feasible for the in situ treatment of contaminated groundwater [7].

Many different types of reactive materials such as hydroxyapatite, ZVI (zero-valent iron), iron oxide and clays have been used to treat metals [7–10]. Clay materials were suggested as a main constituent of backfill materials in PRBs [10]. Those are characterized by elevated plasticity and special sorption capability for heavy metals and radionuclides. However, natural clays are difficult to apply as filling materials in PRB due to their poor hydroconductivity. To complement the drawbacks of the clays, coating of clay minerals by various inorganics; Al, Mn and Fe, has been applied [11–13]. Surface-modification process is generally presented as a way to increase the accessibility of clay layers and plays a key role in determining sorptive and catalytic properties [14]. The surface modification induces high thermal stability, high surface area and essential catalytic activity that are also very important factors to capture the pollutants.

The purpose of this study is to investigate the sorptive removal of Co, Sr and Cs using natural clay (montmorillonite) and coated clays (Mn oxide- and Fe oxide-coated montmorillonites). The single- and bi-solute competitive sorptions were investigated in groundwater system and fitted to several isotherm models. Sorption mechanisms of the metals onto the three materials were discussed. Finally, the optimum sorbent was selected as a backfill material of PRB based on our results.

Materials and methods

Chemicals

Cobalt nitrate ($Co(NO_3)_2{\cdot}6H_2O$, 98+%) and strontium nitrate ($Sr(NO_3)_2$, 99+%) were purchased from Sigma-Aldrich Chemical Co. (Milwakee, WI, USA) and cesium nitrate ($CsNO_3$, 99.9+%) was purchased from Wako Pure Chemical Co. (Japan). Manganese chloride ($MnCl_2{\cdot}4H_2O$, 98+%), manganese sulfate ($MnSO_4{\cdot}H_2O$, 98+%), iron chloride ($FeCl_3{\cdot}6H_2O$, 98+%), iron sulfate ($FeSO_4{\cdot}7H_2O$, 98+%), sodium hydroxide (NaOH, 98+%) were purchased from Duksan Chemical Co. (Korea). MES (2-[*N*-morpholino]ethanesulfonic acid hydrate, 99.5%) buffer was purchased from ACROS Organics (NJ, USA).

Artificial groundwater preparation

Several factors such as dissolved oxygen (DO), temperature, pH and initial concentration of contaminants could affect the groundwater chemistry. To maintain uniform experimental conditions, synthetic groundwater contaminated with Co, Sr and Cs was prepared based on the previous report [15]. The synthetic groundwater was consisted of Na^+, K^+, Mg^{2+}, Ca^{2+}, Cl^-, NO_3^-, SO_4^{2-}, SiO_2, HCO_3^-, etc. [16]. The compositions of the artificial groundwater were listed in detail in Table 1. The pH of synthetic groundwater was maintained at 6 using 0.05 M MES buffer solution. The metal sources in the groundwater contaminated with radionuclides were prepared using non-radioactive metal nitrate for all experiments.

Sorbents preparation

Montmorillonite, Mn oxide-coated montmorillonite (MOCM) and Fe oxide-coated montmorillonite (IOCM) were used as sorbents to treat groundwater contaminated by Co, Sr and Cs. The impurities of the montmorillonite-KSF (Aldrich Chemical Co.) were removed by washing it several times with distilled and deionized water (DI water). The clay suspensions were filtered with 0.2 μm membrane filters (Whatman, cellulose nitrate membrane filter), and the filtrate was examined for impurities using a UV–visible spectrophotometer (Agilent Technology, 8453, USA). The washed montmorillonite was allowed to settle, dried in an oven at 60 °C for 24 h, grounded using a mortar and pestle, passed through a sieve (212 μm) and then stored in a plastic bottle prior to use.

MOCM and IOCM were synthesized by precipitation method. MOCM was prepared with 28 mmol/L of manganese chloride ($MnCl_2{\cdot}4H_2O$) and 14 mmol/L of manganese sulfate ($MnSO_4{\cdot}H_2O$). IOCM was prepared with 28 mmol/L of iron chloride ($FeCl_3{\cdot}6H_2O$) and 14 mmol/L of iron sulfate ($FeSO_4{\cdot}7H_2O$) [12, 13, 17]. Briefly, 15 g of the washed montmorillonite was stirred in 400 mL of the metal solutions at 160 rpm using a mechanical overhead stirrer. 100 mL of NaOH solution (6 mol/L for MOCM and 5 mol/L for IOCM) was added dropwise to precipitate Mn or Fe oxides on the surface of the montmorillonite. The reaction temperature was maintained at 60 °C for 90 min. After precipitation, the supernatant was decanted and the mixtures were exposed to air to facilitate oxidation of the Mn or Fe hydroxide to a mixture of hydrated Mn oxides or Fe oxides. The metal coated-montmorillonites were air-dried for 2–3 days and then dried in an oven at 60 °C for 2 days. They were grounded using a mortar and pestle, passed through a 212 μm sieve (US standard mesh), and then stored in plastic bottles prior to use.

Table 1 The artificial groundwater composition

	Concentration (mg L^{-1})
Na^+	20.0
K^+	2.0
Mg^+	5.0
Ca^{2+}	30.0
Cl^-	15.0
SO_4^{2-}	35.0
HCO_3^-	60.0
pH	6.0
T(°C)	25.0

Characterization of the sorbents

The physicochemical properties of the sorbents were characterized. Specific surface area was measured from N_2 sorption/desorption isotherm fitted by the Brunauer-Emmett-Teller (BET) model. Pore size distribution, pore volume and pore diameter (micro-, meso-, and/or macropores) determined by BJH (Barrett-Joyner-Halenda) sorption model using a specific surface area analyzer (UPA-150, Microtrac, USA). Scanning electron microscopy (SEM, S-4200, HITACHI, Japan) with energy dispersive X-ray (EDX, Horiba, E-MAX EDS detector) analysis for studying surface morphology and chemical composition of the sorbents were also performed. X-ray diffraction (XRD) patterns were obtained using Cu $K\alpha$ radiation ($\lambda = 1.54$ Å) on multi purpose X-ray diffractometer (X'pert PRO MRD, PANalytical, The Netherlands). XRD peaks were measured in the range from 1° to 12° of 2θ values with a step size of 0.02 and a step time of 1.5 s. Cation exchange capacity (CEC) of the sorbents was measured by the sodium acetate method [18]. The sample was mixed with an excess of 1 N of sodium acetate solution, resulting in an exchange of the added cations in substitute for the matrix cations. Subsequently, the sample was washed with isopropyl alcohol (99.5%). 1 N of ammonium acetate solution was then added, which replaces the sorbed sodium with ammonium. The concentration of displaced sodium was then determined by inductively coupled plasma-optical emission spectrometer (ICP-OES, Optima 2100DV, PerkinElmer Co., USA). The pH of point of zero charge (pH_{PZC}) of the sorbents was determined by batch technique [19]. 0.5 g of montmorillonite, MOCM and IOCM and with 30 mL of 0.1 M KNO_3 solution as an inert electrolyte were mixed in 50 mL conical tubes (Polyethylene, SPL Co., Korea). The initial pHs (from 2 to 10) of the solution were adjusted by adding 0.1 N HNO_3 or 0.1 N KOH. The samples were shaken for 24 h at 200 rpm and 25 °C to reach equilibrium. The final pH of the solution was measured by a pH meter (720 A+, Thermo

Orion, USA). In addition, the XRD peaks of all sorbents after sorption were also analyzed to find out the changes in their crystalline features.

Sorption experiment

Single-solute sorption experiments were conducted using 50 mL conical tubes containing 2.0 g of sorbents. The pH of the sorbent was controlled to 6.0 by rinsing the sorbent two times with 0.05 M MES buffer solution before performing all experiments. The tubes containing sorbents were filled with the metal solutions and the headspace was minimized to exclude the effect of carbon dioxide in the air. Then, the vials were placed on a shaking incubator and mixed for 48 h. Preliminary kinetic experiments showed that sorption equilibrium was reached within 4 h (data not shown). However, sorption experiments were conducted for 48 h to ensure sorption equilibrium. To obtain sorption isotherm, seven to ten different initial concentrations (Co and Cs: 1–50 mM and Sr: 1–30 mM) were prepared. The pH of stock solution was also controlled to 6.0 using 0.05 M MES buffer. Preliminary experiments showed that the buffer has no effect on metal sorption. Wolff-Boenisch and Traina [20] also reported that no detectable complexation reactions occurred between the metals and MES buffer. After sorption experiments, the vials were centrifuged and the supernatant was filtered through 0.45 μm syringe filter (Whatman, cellulose nitrate membrane filter). The aqueous phase concentrations of the metals were analyzed by the ICP-OES. The solid phase equilibrium concentrations were calculated from the mass balance by assuming that all concentration changes in solution phase resulted from sorption onto the solid phase. All experiments were run in duplicate.

Bi-solute systems (Co/Sr, Sr/Cs and Co/Cs) were prepared by mixing each metal solution of the same molar concentration (1–30 mM) in a 1:1 volume ratio. Bi-solute competitive sorption experiments were conducted in the same manner as were in the single-solute sorption experiments. The aqueous phase samples in the mixture were analyzed by the ICP-OES.

Sorption models

Single-solute sorption models

The Freundlich, Langmuir and Dubinin-Radushkevich (D-R) models were applied to explain the sorption mechanism of the metals onto the sorbents in single-solute system.

The Freundlich model is often used to describe sorption onto heterogeneous surface:

$$q = K_{\mathrm{F}} C^{N_F} \tag{1}$$

where C (mmol/L) is the aqueous-phase equilibrium concentration, q (mmol/g) is the solid-phase equilibrium concentration, and K_{F} [(mmol/g)/(mmol/L)^{N_F}] and N_{F} (−) are Freundlich sorption coefficient and the Freundlich exponent, respectively.

The Langmuir model is described by a limiting maximum sorption capacity that is related to monolayer coverage of surface sites. The Langmuir model is written as:

$$q = \frac{q_{\mathrm{mL}} b_{\mathrm{L}} C}{1 + b_{\mathrm{L}} C} \tag{2}$$

where q_{mL} (mmol/g) and b_{L} (L/mol) are the Langmuir parameters representing maximum sorption capacity and site energy factor, respectively.

The Dubinin-Radushkevich isotherm (D-R) is more general than the Langmuir isotherm because it does not assume a homogeneous surface or constant sorption potential [3]. The D-R isotherm is applied to distinguish between the physical and chemical sorptions.

$$q = q_{\mathrm{mD}} \exp\left(-\beta\varepsilon^2\right) = q_{\mathrm{mD}} \exp\left[-\beta\left(RT\ln\left(1 + \frac{1}{C}\right)\right)^2\right] \tag{3}$$

where β is a constant related to the mean free energy of sorption per mole of the sorbate (mol^2/J^2), q_{mD} is the theoretical saturation capacity (mmol/g) and ε is the Polanyi potential, which is equal to $RT\ln(1 + 1/C)$, where R (J/mol-K) is the gas constant and T (K) is the absolute temperature. The constant β gives an idea about the mean free energy E (J/mol) of the sorption per molecule of the sorbate when it is transferred to the surface of the solid from infinity in the solution and this energy can be computed using the following relationship [21].

$$E = \frac{1}{(2\beta)^{1/2}} \tag{4}$$

The sorption model parameters were determined by using a commercial software package, Table Curve 2D (Version 5.1, SYSTAT Software, Inc.).

Bi-solute competitive sorption models

The Sheindorf-Rebhun-Sheintuch (SRS) model, the competitive Langmuir model (CLM) and the P-Factor model were applied to explain the sorption mechanism of the metals onto the sorbents in bi-solute systems.

The Sheindorf-Rebhun-Sheintuch (SRS) model was developed to describe competitive sorption assuming that the single-component sorption follows the Freundlich model [22]. The derivation of SRS equation is based on the assumption of an exponential distribution of sorption

energies for each component. A general form of the SRS model can be written as

$$q_{m,i} = \frac{K_{F,i} C_{m,i}}{\sum_{j=1}^{2} \left(\alpha_{i,j} C_{m,j}\right)^{1-N_{F,i}}} \quad (5)$$

where subscripts i and j denote metal solutes i and j, $q_{m,i}$ (mmol/g) and $C_{m,i}$ (mmol/L) are the solid-phase and the liquid-phase equilibrium concentration of a solute i in bi-solute competitive sorption, respectively. $\alpha_{i,j}$ is a dimensionless competition coefficient for the sorption of solute i in the presence of solute j. The parameters $K_{F,i}$ and $N_{F,i}$ are the Freundlich parameters obtained from single-solute system. By definition, $\alpha_{i,j} = 1$ when $i = j$. If there is no competition, that is, $\alpha_{i,j} = 0$ for all $j \neq i$.

The competitive Langmuir model (CLM) was used to analyze bi-solute competitive sorption behaviors [23]. The CLM is an extended form of the Langmuir model which allows predictions of the amount of a solute i sorbed per unit weight of an sorbent, $q_{m,i}$ in the presence of other solutes.

$$q_{m,i} = \frac{q_{mL,i} b_{L,i} C_{m,i}}{1 + \sum_{j=1}^{2} b_{L,j} C_{m,j}} \quad (6)$$

where $q_{mL,i}$ (mmol/g) and $b_{L,i}$ (L/mmol) are the parameters determined by fitting the Langmuir model to the single-solute sorption data of solute i.

The P-factor model was used to analyze bi-solute competitive sorption behaviors [24]. This model is based on a simplified approach that can be used to compare and correlate single-solute sorptions with those of the multi-component systems by introducing a "lumped" capacity factor P_i [25]:

$$P_i = \frac{q_{mL,i}}{q^*_{mL,i}} \quad (7)$$

where $q_{mL,i}$ is the sorbent monolayer capacity for component i in single-solute component system, while $q^*_{mL,i}$ is that in bi-solute component system. This model assumes a Langmuir isotherm; hence, for each component i, the bi-component isotherm equation is described as:

$$q_{m,i} = \frac{1}{P_i} \frac{b_{L,i} q_{mL,i} C_{m,i}}{1 + b_{L,i} C_{m,i}} \quad (8)$$

Results and discussion

Sorbents characteristics

SEM images and EDS peaks of the sorbents were presented in Figs. 1 and 2, respectively. The surface images of MOCM and IOCM are similar to that of montmorillonite. SEM images revealed a birnessite structure of Mn oxides on MOCM, which was featured by a plate-like-crystal structure. The small particles appeared on the surface of IOCM might be iron oxide formed. The EDS peaks of the sorbents confirmed that Mn or Fe oxides were present in the modified montmorillonites (Fig. 2). Mn loading in MOCM and Fe loading in IOCM were 7.15 and 10.63 wt%, respectively.

The XRD patterns of montmorillonite, MOCM and IOCM before and after Cs sorption were presented in Fig. 3. The d_{001}-spacing peaks indicating the interlayer distance in untreated and the modified clays were 12.13 Å at 7.13° in pristine montmorillonite, 13.62 Å at 6.48° in MOCM and 12.85 Å at 6.87° in IOCM, respectively. The basal spacing value of pristine montmorillonite (B3378, Sigma-Aldrich, USA) was 12.13 Å reported by Yu et al. [26] which were similar to our result. Given that d_{001}-spacing peak in the pristine montmorillonite, surface coating of montmorillonte with Mn or Fe oxide only slightly increased the interlayer spacing. The XRD peak of IOCM suggested that goethite and maghemite were formed in the surface of the IOCM. Oliverira et al. [13] reported that goethite was preferentially formed in the clay/Fe oxide composite.

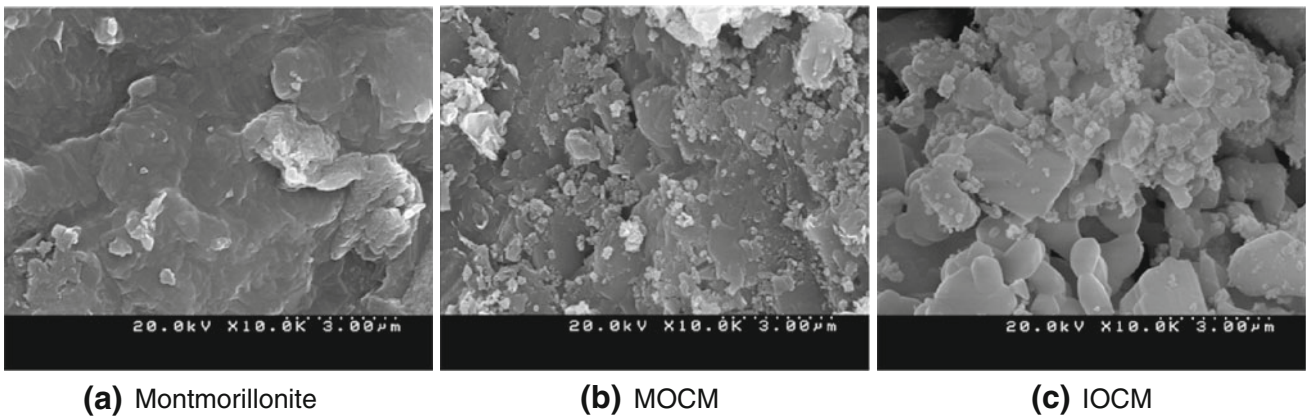

Fig. 1 SEM images of **a** montmorillonite, **b** MOCM and **c** IOCM

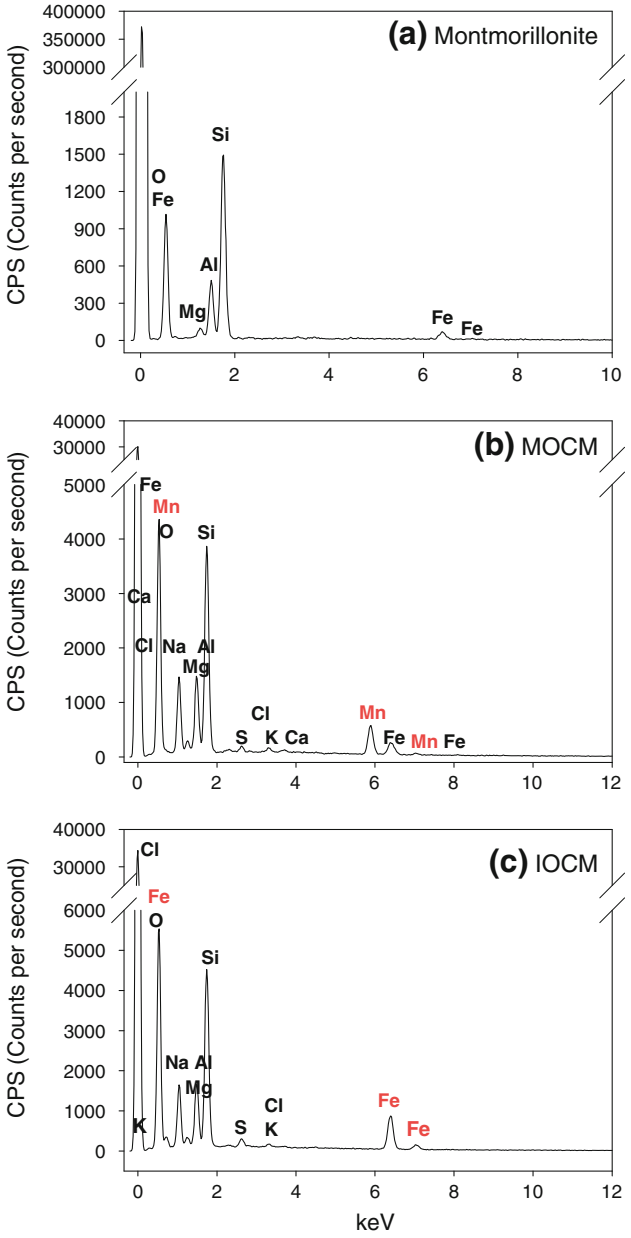

Fig. 2 SEM-EDX analyses of the sorbents used in this study

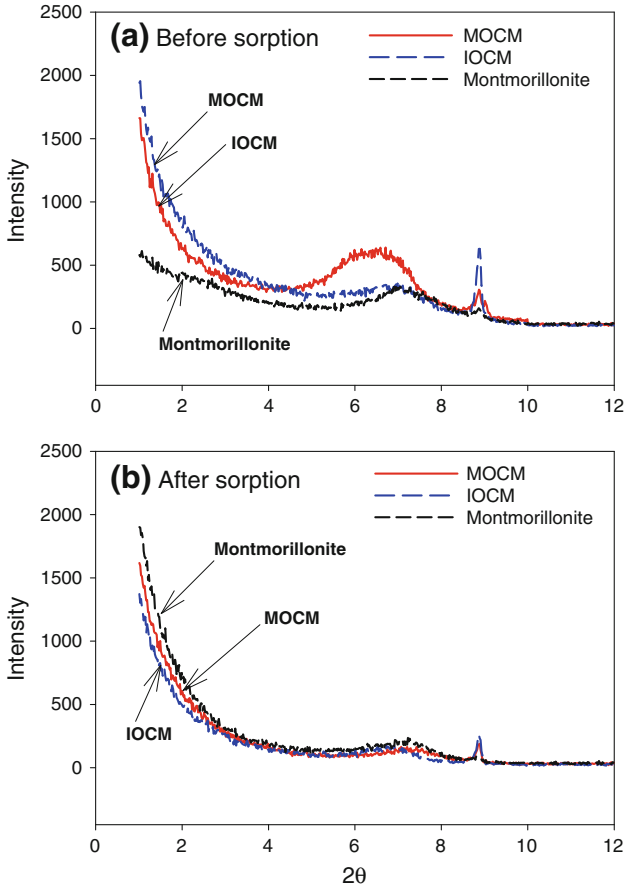

Fig. 3 XRD analyses of the sorbents used in this study. **a** before and **b** after Cs sorption

Table 2 The physicochemical characteristics of the sorbents used

	Sorbents		
	Montmorillonite	MOCM	IOCM
CEC (meq/100 g)	52.73	84.89	82.45
pH_{PZC}	3.0	4.1	9.0
BET Surface area (m^2/g)	13.93	6.144	2.201
Total pore volume (cm^3/g)	0.0253	0.0192	0.0069
Volume of micropores (cm^3/g)	0.00046	0.00035	0.00071
Fraction of micropore volume (%)	1.84	1.84	10.2
Average pore diameter (nm)	7.26	12.51	12.61

Surface area, pore volume and diameter, CEC and pH_{PZC} of the sorbents used in this study were summarized in Table 2. The montmorillonite, MOCM and IOCM showed the surface area ranged from 2 to 13 m^2/g. The average pore diameter was in the order of MOCM (12.51 nm) > IOCM (12.61 nm) > montmorillonite (7.26 nm). It was confirmed that the Mn or Fe oxide coating on the clay affected not only morphology, but also porosity and pore size distribution of the clay and thus it could influence the sorption properties [27]. CEC of MOCM (84.89 meq/100 g) and IOCM (82.45 meq/100 g) were similar each other but were higher than that of the unmodified montmorillonite (52.73 meq/100 g). Unlike our data, Ijagbemi et al. [28] reported that CEC of montmorillonite was 89 meq/100 g from extraction with ammonium acetate. The pH_{PZC} of montmorillonite and MOCM was 3.0 and 4.1, respectively. Ijagbemi et al. [28] reported that the pH_{PZC} of montmorillonite was 3.6 and that of hydous manganese oxide (HMO)-coated clay was 2.8 which is similar to the pH_{PZC} of HMO powder. They

reported that HMO-coated clay behaved similar to HMO powders on the interface between liquid and solid surface. The pH_{PZC} of ICOM (pH 9) was similar to that of goethite (pH 8) reported by Nachtegaal and Sparks [29]. These results indicate that metal oxide coating onto montmorillonite play an important role in the surface charge behavior and physical metal sorption.

Speciation of metals

The metal speciation of Co, Sr and Cs at all pH ranges considering the chemical composition of the groundwater were predicted by MINEQL+ (version 4.0) for Windows (Environmental Research Software, USA) (Fig. 4). Co^{2+} was the dominant Co species at pH below 7. At pH higher than 7, cobalt precipitates as $Co(OH)_2$. Sr existed mostly as Sr^{2+} and a little $Sr(NO_3)^+$ at almost all pH ranges. However, $Sr(OH)^+$ began to form at pH 11. In contrast to Co and Sr, Cs mainly exists as Cs^+ and no precipitate is formed at all pH ranges, indicating that Cs does not combine with any anions included in the groundwater. It was noted that Co, Sr and Cs sorptions are not affected by precipitation at pH 6 in both single- and bi-solute sorptions.

Single-solute sorption

Sorption isotherm explains the relationship between the amount of sorbate on the sorbent and the concentration of dissolved sorbate in the liquid at equilibrium. Sorptions of the heavy metals onto the sorbents were shown in Figs. 5 (Co), 6 (Sr), 7 (Cs) and the model parameters were summarized in Tables 3 (Freundlich), 4 (Langmuir) and 5 (D-R), respectively. All sorbents showed higher sorption capacity of Co, Sr and Cs indicating strong sorbate-sorbent interactions. The sorption capacity was in the order of MOCM > IOCM ≈ montmorillonite for Co and Sr, and montmorillonite > MOCM > IOCM for Cs.

The Freundlich, Langmuir, D-R models were fitted to the sorption data. The Freundlich model fitted the sorption data very well ($0.98 < R^2 < 0.99$) (Table 3). The Freundlich sorption constant, K_F, indicates the sorption capacity of the sorbents. The K_F values were in the order of Cs > Co > Sr in all sorbents. The Freundlich exponent, N_F, is a measure of the derivation from linearity of the sorption. If a value for N_F is equal to unity, the sorption is linear. If N_F value is above 1, this implies that sorption process is chemical, but if N_F value is below 1, sorption is favorable for a physical process. The N_F values of the three sorbents at equilibrium ranged between 0.24 and 0.54 represented that sorption was favorable and highly non-linear [30].

The Langmuir model was also fitted to the sorption data well ($0.97 < R^2 < 0.99$) (Table 4). The q_{mL} values of

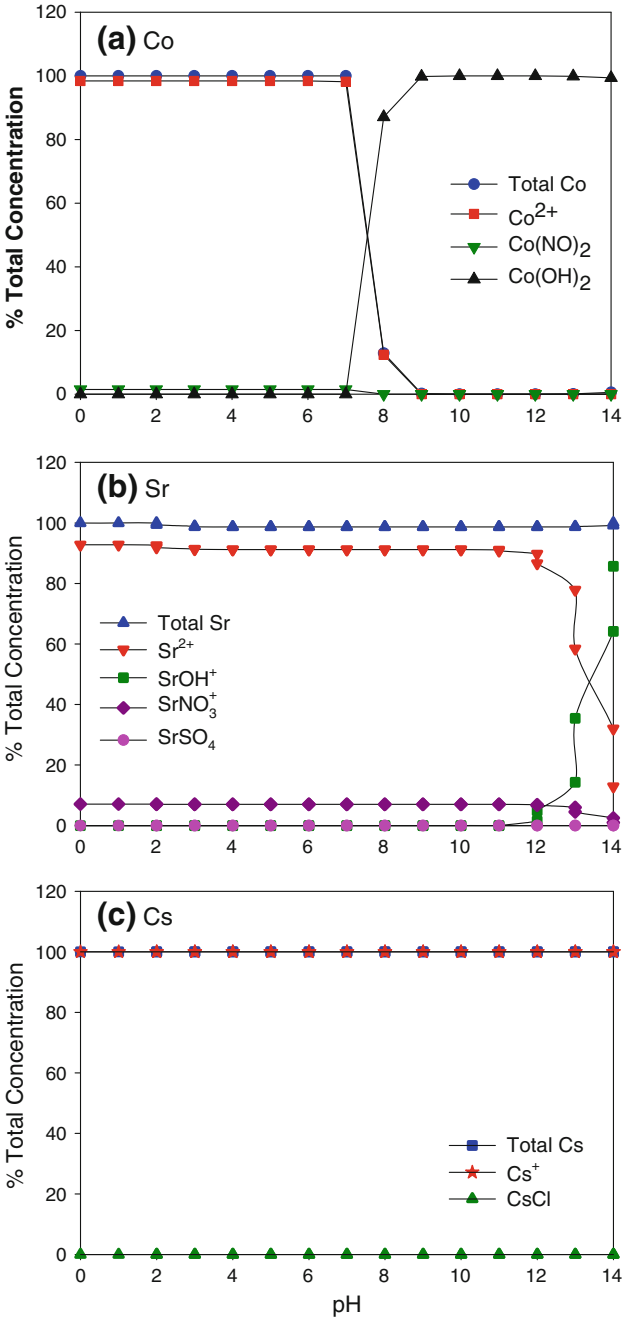

Fig. 4 % total concentration of **a** Co, **b** Sr and **c** Cs species at different pH levels

montmorillonite and metal oxide-coated montmorillonites were in the order of Cs > Co > Sr. The q_{mL} values of Co were in the order of MOCM (0.37 mmol/g) > montmorillonite (0.27 mmol/g) > IOCM (0.22 mmol/g). For Sr, the q_{mL} values of MOCM (0.28 mmol/g) and IOCM (0.21 mmol/g) were higher than that of montmorillonite (0.19 mmol/g). Unlike Co and Sr, the q_{mL} values of Cs were in the order of montmorillonite (1.11 mmol/g) > MOCM (0.68 mmol/g) > IOCM (0.62 mmol/g). Bhattacharyya and

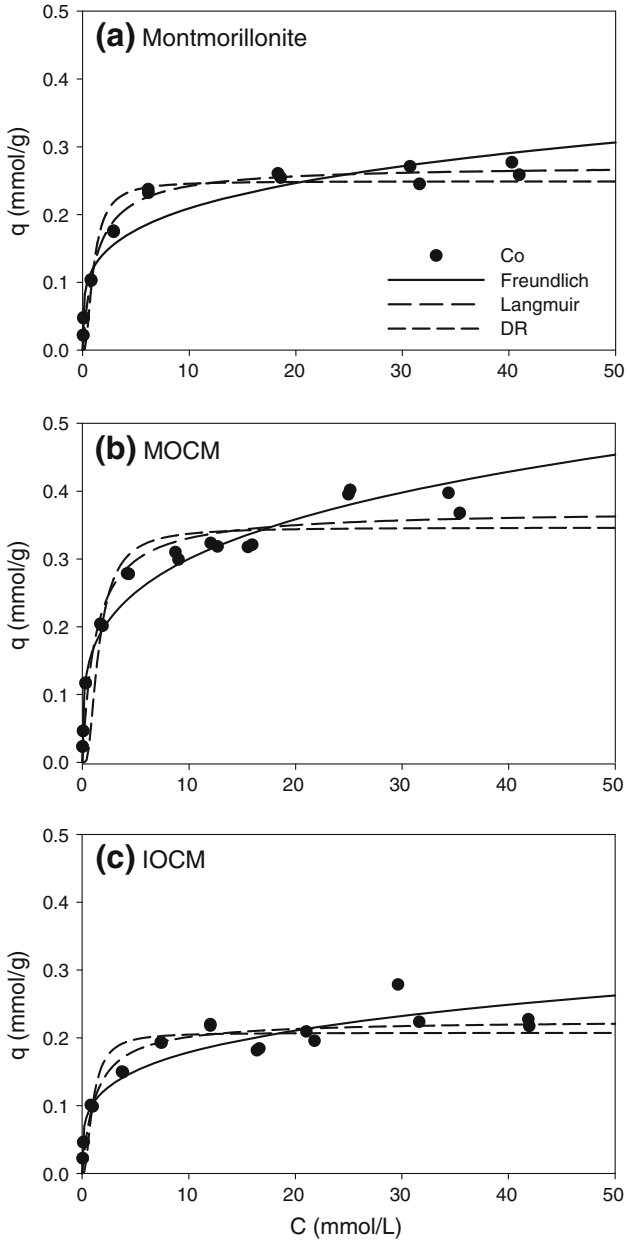

Fig. 5 Single-solute sorption of Co onto sorbents. *Lines* represent sorption models

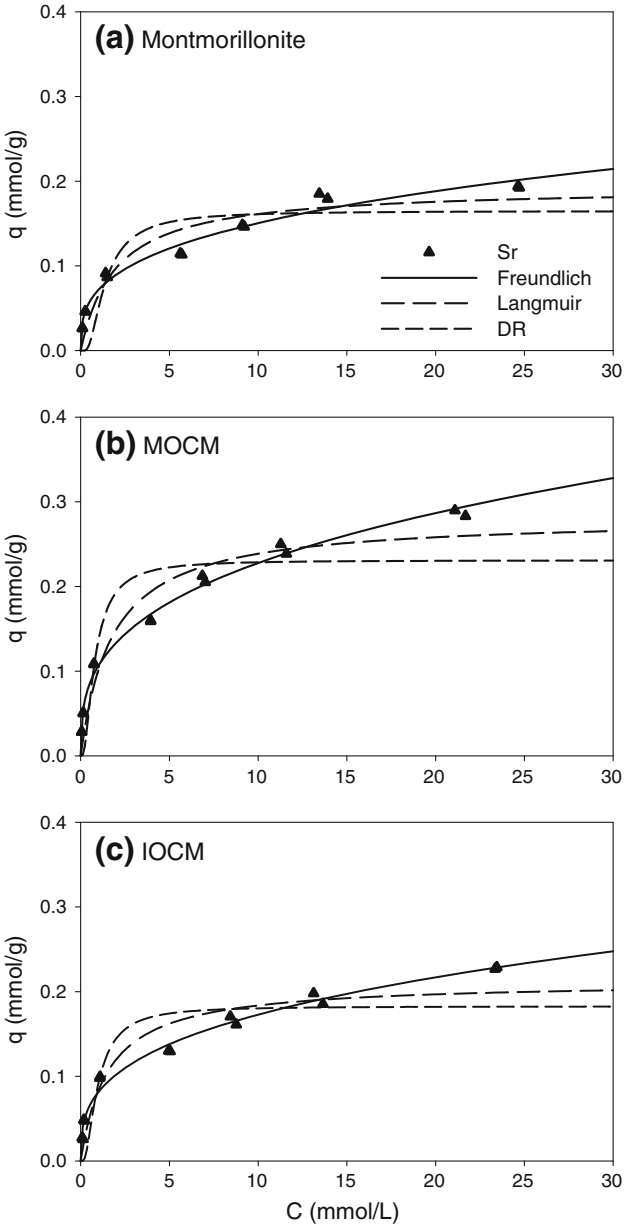

Fig. 6 Single-solute sorption of Sr onto sorbents. *Lines* represent sorption models

Gupta [31] reported that the q_{mL} value of Co on montmorillonite at pH 5.8 was 28.6 mg/g (0.48 mmol/g) higher than our result. The difference of the q_{mL} value was attributed by the difference in the compositions of montmorillonite used (Aldrich montmorillonite KSF, vs. SWy-2, Source Clay Minerals Resository, USA). Wen et al. [32] also reported that the q_{mL} value of Cs on Na-montmorillonite (from Zhejiang Sanding Group Co. Ltd., China) was 0.44 mmol/g at 293 K, pH 6.0, I = 0.01 M NaCl and m/V = 0.5 g/L. The value was higher than that of our result. This is because the experimental conditions such as initial concentration of Cs and ionic strength in the single-solute sorption was different from ours. Galamboš et al. [33] reported that the q_{mL} value of Cs on montmorillonite (Aldrich montmorillonite K10) was 0.28 mmol/g. Ararem et al. [34] reported that the q_{mL} value of Cs on the mixture with iron pillared montmorillonite (Fe-PILM) and goethite (α-FeOOH) (mass ratio of Fe-PILM/goethite = 4) was 0.43 meq/g, lower than that of our IOCM due to different preparation method of iron containing montmorillonite, initial concentration of Cs solution on sorption and so on. The fundamental characteristic of Langmuir isotherm can be expressed in terms of a dimensionless constant, separation factor $R_L(-)$, that describes the type of isotherm [35].

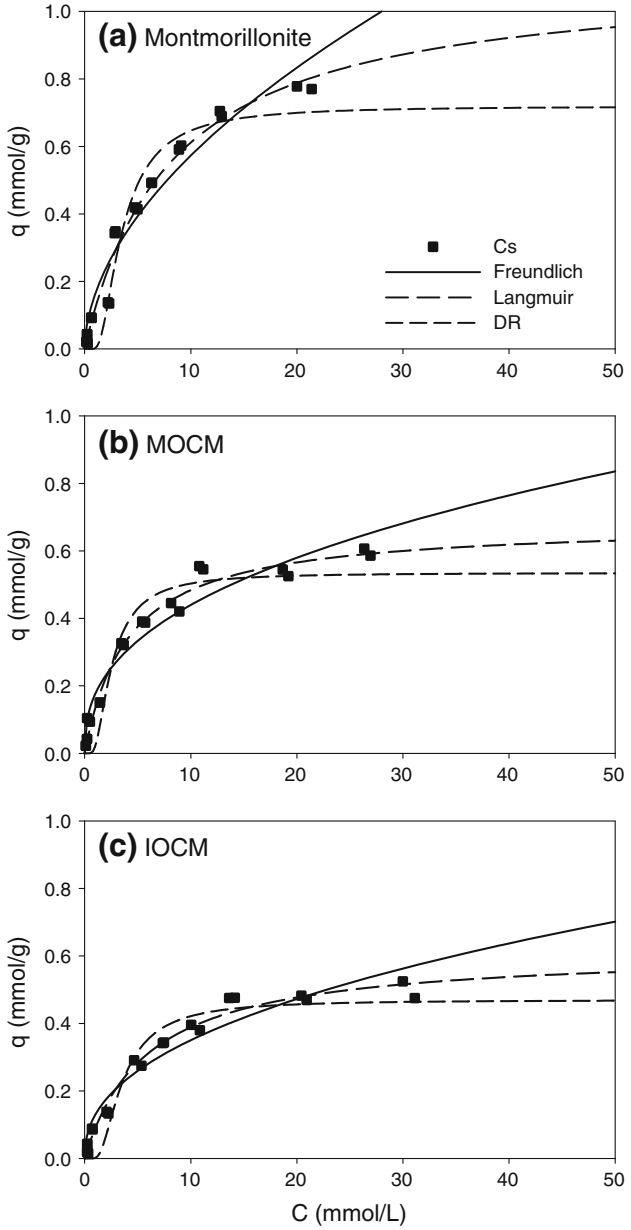

Fig. 7 Single-solute sorption of Cs onto sorbents. *Lines* represent sorption models

$$R_L = \frac{1}{1 + b_L C_0} \tag{9}$$

where b_L is the Langmuir constant and C_0 is the initial concentration of heavy metal solution. The value of R_L indicates the type of isotherm to be unfavorable ($R_L > 1$), linear ($R_L = 1$), favorable ($0 < R_L < 1$) or irreversible ($R_L = 0$). All R_L values were between 0.02 and 0.21 (Table 4) indicating that sorptions of Co, Sr and Cs onto the sorbents are favorable [35].

The parameters of Dubinnin-Radushkevich (D-R) model were listed in Table 5. The D-R model also fitted the sorption data well ($0.94 < R^2 < 0.98$). The order of increase in q_{mD} was the same as the q_{mL} of Langmuir model (Table 4). The value of mean free energy E in D-R model indicates whether sorption mechanism is ion-exchange or physical sorption. If the E is between 8 and 16 kJ/mol, the sorption system progresses by ion-exchange, while for the value of $E < 8$ kJ/mol, the sorption system is of a physical nature. For the value of $E > 16$ kJ/mol, the sorption occurs by means of chemical sorption [3]. In this study, the E values calculated using Eq. 4 were less than 8 kJ/mol indicating that sorptions of Co, Sr and Cs on the sorbents followed physical sorption. The Freundlich exponent, N_F, in Freundlich model as well as the value of mean free energy E, in D-R model implicates that the mechanism of sorption was physical. Başçetin and Atun [36] explained Sr sorption onto montmorillonite using D-R models. The ranges of E values in D-R model were 8–16 kJ/mol when the initial Sr^{2+} concentrations are 1×10^{-6}–1×10^{-2} M. Their results were different from ours. This is because many factors such as sorbent type (Aldrich montmorillonite KSF (CEC = 52.73 meq/100 g), vs. Turkish montmorillonite (CEC = 246 meq/100 g)), ion-strength, pH, initial concentration and contact time might affect sorption mechanisms.

In the single-solute sorption, we found that; (i) Fe or Mn oxide-coated montmorillonite had higher sorption capacity of Co and Sr than untreated montmorillonte (except Co sorption onto IOCM), and (ii) untreated montmorillonite

Table 3 Freundlich model parameters for single-solute sorption of Co, Sr and Cs at pH 6.0

Solute	Sorbent	K_F [(mmol/g)/(mmol/L)^{N_F}]	N_F (−)	R^2	SSE
Co	Montmorillonite	0.1211 ± 0.0100	0.2372 ± 0.0270	0.9809	0.0288
	MOCM	0.1660 ± 0.0083	0.2571 ± 0.0176	0.9926	0.0247
	IOCM	0.1028 ± 0.0083	0.2395 ± 0.0273	0.9824	0.0245
Sr	Montmorillonite	0.0719 ± 0.0038	0.3215 ± 0.0203	0.9950	0.0099
	MOCM	0.1063 ± 0.0037	0.3314 ± 0.0142	0.9974	0.0099
	IOCM	0.0815 ± 0.0037	0.3268 ± 0.0176	0.9961	0.0097
Cs	Montmorillonite	0.1648 ± 0.0175	0.5411 ± 0.0430	0.9820	0.0633
	MOCM	0.1756 ± 0.0163	0.3988 ± 0.0348	0.9821	0.0532
	IOCM	0.1296 ± 0.0142	0.4316 ± 0.0393	0.9809	0.0479

Table 4 Langmuir model parameters for single-solute sorption of Co, Sr and Cs at pH 6.0

Solute	Sorbent	q_{mL} (mmol/g)	b_L (L/mmol)	R^2	SSE	R_L*
Co	Montmorillonite	0.2726 ± 0.007	0.2372 ± 0.027	0.9944	0.0156	0.078
	MOCM	0.3718 ± 0.013	0.8104 ± 0.172	0.9895	0.0247	0.024
	IOCM	0.2263 ± 0.009	0.8049 ± 0.211	0.9854	0.0224	0.024
Sr	Montmorillonite	0.1931 ± 0.014	0.5106 ± 0.162	0.9799	0.0197	0.061
	MOCM	0.2813 ± 0.019	0.5635 ± 0.172	0.9818	0.0262	0.056
	IOCM	0.2119 ± 0.014	0.6506 ± 0.209	0.9791	0.0225	0.049
Cs	Montmorillonite	1.1095 ± 0.073	0.1229 ± 0.018	0.9921	0.0420	0.213
	MOCM	0.6821 ± 0.027	0.2445 ± 0.031	0.9940	0.0308	0.112
	IOCM	0.6168 ± 0.024	0.1705 ± 0.020	0.9951	0.0243	0.164

*Calculated at $C_0 = 50$ mM for Co and Cs at $C_0 = 30$ mM for Sr, respectively

Table 5 Dubinin-Radushkevich model parameters for single-solute sorption of Co, Sr and Cs at pH 6.0

Solute	Sorbent	q_{mD} (mmol/g)	β (mol^2/J^2 × 10^{-8})	R^2	SSE	E (kJ/mol)
Co	Montmorillonite	0.2490 ± 0.010	24.723 ± 5.5902	0.9815	0.0284	1.422
	MOCM	0.3718 ± 0.013	46.637 ± 15.647	0.9682	0.0511	1.035
	IOCM	0.2074 ± 0.009	23.514 ± 7.1398	0.9727	0.0306	1.458
Sr	Montmorillonite	0.1649 ± 0.012	40.037 ± 16.853	0.9491	0.0314	1.118
	MOCM	0.2310 ± 0.016	17.705 ± 6.7708	0.9541	0.0416	1.681
	IOCM	0.1826 ± 0.013	23.148 ± 10.091	0.9503	0.0347	1.470
Cs	Montmorillonite	0.7195 ± 0.028	189.96 ± 24.059	0.9825	0.0625	0.513
	MOCM	0.5351 ± 0.022	108.09 ± 22.713	0.9781	0.0589	0.680
	IOCM	0.4696 ± 0.019	193.66 ± 37.815	0.9803	0.0487	0.508

showed higher sorption capacity of Cs than the coated montmorillonite.

The sorption mechanism of metal ions on montmorillonite may be explained by two aspects: first, chemical binding reaction between the metal ions and the respective surface functional groups (hydroxyl groups), forming inner-sphere surface complexes; second, electrostatic binding reaction between the metal ions and the negatively charged sites (or permanent negatively charged sites) of montmorillonite, forming outer-sphere complexes at a certain distance from the surface. The former may be described as specific sorption, which is characterized by more selective and less reversible reactions; the latter may be described as nonspecific sorption (or ion exchange), which is characterized by less selective and rather weak and reversible reactions [37]. This sorption mechanism can be changed through the treatment of Fe or Mn oxide coating onto the clay surface, which influences the sorbent's properties, for example, specific surface area, porosity, particle size, surface charge of the clays. Therefore, the surface groups exposed by dispersed 'oxides' probably play a key role in determining the promising sorptive properties of the coated clays [38].

The metal oxide-coated montmorillonites showed higher sorption capacities of Co and Sr than montmorillonte. The sorption phenomenon in metal oxide-coated montmorillonites could be altered by the change of surface charge, which could enhance the sorption of Co and Sr. There exist three exchange sites, i.e., surface proton, Mn^{2+} and Mn^{3+} in the Mn oxide lattice. The Co sorption onto the MOCM could be mainly due to specific chemical interaction sites for Mn^{2+} and Mn^{3+} even by releasing Mn ions into solution from its disordered lattice, as well as surface proton, H^+ [39]. Sr could be sorbed by exchange with surface protons and the site of Mn^{2+} except for the site of Mn^{3+}. This is the reason why the sorption capacity of Co and Sr in MOCM was higher than those of the pristine montmorillonite. The IOCM showed higher sorption capacity of Sr than montmorillonite. This might be caused by the formation of extra sorption sites created by the sorption of Fe oxide, i.e., goethite and maghemite particles onto montmorillonite. However, the sorption capacity of Co and Sr onto IOCM was lower than that onto MOCM. It was reported that the pH_{PZC} of MOCM and IOCM were around pH 4 and 9, respectively. This means that the surface of the MOCM was negatively charged, while that of the IOCM

was positively charged at pH 6. This positively charged surface of the IOCM might repel the cations (Co and Sr) away from the surface and thus less Co and Sr sorptions occurred.

Among the three metals, the maximum sorption capacities of the untreated montmorillonite were in the order of Cs $\gg$ Co > Sr. Besides, Cs sorption capacity of the untreated montmorillonite was higher than those of the metal oxide-coated montmorillonites. In montmorillonite, both electrostatic binding reaction between the metal ions on the negatively charged sites such as the surfaces parallel to the aluminosilicate sheets and interlayer and chemical binding reaction between the metal ions and the respective surface hydroxyl groups at the frayed edges were considered as the main mechanism to remove metals in the solution [37, 39]. The preferential retention of Cs in clay materials is believed to take place in highly selective sites located at the frayed edges of the clay particles. This preference has been attributed to the large ionic radius and uncomplexing nature of Cs, but most importantly to its low hydration energy [40]. Thus Cs is fixed much more tightly than Co and Sr at the frayed edges as the specific sorption [41]. Compared to Co (4.23 Å) and Sr (4.12 Å), Cs (3.29 Å) has a smaller Stokes radius of the hydrated ion [42]. Therefore, Cs sorption onto the untreated montmorillonite occurred by both mechanisms, i.e., ion exchange and surface complexation while Co or Sr sorption occurred by ion exchange only. Yu et al. [26] also reported that the Co sorption onto pristine montmorillonite may be attributed to electrostatic and Coulombic attraction. The metal-coating on the surface of the montmorillonite could considerably reduce Cs sorption by covering the preferential sorption sites.

The XRD pattens of Cs-sorbed montmorillonite, MOCM and IOCM were presented in Fig. 3b. The basal spacing (d_{001}) of Cs-sorbed montmorillonite, MOCM and IOCM showed similarly 9.976 Å at 8.857°, 9.971 Å at 8.861° and 9.984 Å at 8.849°s, respectively. Compared to the original sorbents before sorption, the basal spacing of Cs-sorbed sorbents decreased. This supports that Cs sorption onto the surface of montmorillonite, MOCM and IOCM occurs via ionic exchange or nonspecific surface sorption [43]. Iijima et al. [44] also reported that the basal spacing of montmorillonte decresed after Cs sorption and with increasing Cs concentration.

Bi-solute competitive sorption

Bi-solute competitive sorptions of Co/Sr, Co/Cs and Cs/Sr onto the sorbents were analyzed by the Langmuir model (Table 6). The maximum sorption capacity (q^*_{mL}) and sorption affinity (b^*_L) in bi-solute system was compared with those in single-solute system (q_{mL} and b_L). The q^*_{mL} of bi-solute competitive sorption (Table 6) was less than that of single-solute sorption (Table 4) as expected by coexistence of competing metals. Especially, Cs sorption onto the three sorbents in bi-solute systems was strongly influenced by competition.

The effect of bi-solute competition on the sorption of the metals can be also analyzed by the ratios of the sorption

Table 6 Langmuir model parameters for bi-solute competitive sorption of Co, Sr and Cs at pH 6.0

Sorbent	Solute	q^*_{mL} (mmol/g)	b^*_L (L/mmol)	R^2	SSE
Montmorillonite	Co/Sr	0.1438 ± 0.0126	0.3130 ± 0.1011	0.9781	0.0143
	Sr/Co	0.1258 ± 0.0137	0.4883 ± 0.2332	0.9489	0.0214
MOCM	Co/Sr	0.2553 ± 0.0148	0.6469 ± 0.1695	0.9860	0.0211
	Sr/Co	0.2398 ± 0.0264	0.1877 ± 0.0619	0.9763	0.0211
IOCM	Co/Sr	0.1922 ± 0.0119	0.3960 ± 0.0961	0.9877	0.0144
	Sr/Co	0.2077 ± 0.0250	0.1713 ± 0.0607	0.9731	0.0194
Montmorillonite	Cs/Sr	0.4343 ± 0.0326	0.3713 ± 0.0928	0.9862	0.0299
	Sr/Cs	0.0936 ± 0.0069	3.4471 ± 1.6686	0.9539	0.0180
MOCM	Cs/Sr	0.4238 ± 0.0163	0.4826 ± 0.0638	0.9953	0.0178
	Sr/Cs	0.1184 ± 0.0069	2.7238 ± 1.1032	0.9738	0.0164
IOCM	Cs/Sr	0.4943 ± 0.0731	0.2975 ± 0.1103	0.9674	0.0454
	Sr/Cs	0.1279 ± 0.0096	1.1780 ± 0.5045	0.9689	0.0178
Montmorillonite	Cs/Co	0.3970 ± 0.0242	0.3787 ± 0.0924	0.9847	0.0322
	Co/Cs	0.2251 ± 0.0256	0.1433 ± 0.0580	0.9602	0.0291
MOCM	Cs/Co	0.5447 ± 0.0327	0.2080 ± 0.0364	0.9908	0.0289
	Co/Cs	0.2960 ± 0.0143	0.4411 ± 0.1170	0.9843	0.0279
IOCM	Cs/Co	0.5784 ± 0.0523	0.1241 ± 0.0299	0.9821	0.0409
	Co/Cs	0.2290 ± 0.0111	0.3974 ± 0.1044	0.9842	0.0219

q^*_{mL} and b^*_L indicates q_{mL} value and b_L value for bi-solute competitive sorption, respectively

capacity of one metal in the presence of other metal, q^*_{mL}, to the sorption capacity of corresponding metal in single-solute solution, q_{mL}, as summarized in Table 7. Almost all of the $q_{mL,1}/q_{mL,2}$ ratios as well as $q^*_{mL,1}/q^*_{mL,2}$ ratios were higher than unity indicating the predominant sorption of Co in Co/Sr, Cs in Cs/Sr and Cs in Cs/Co onto all sorbents regardless of competition. However, Co in the Co/Sr system onto IOCM was not. Sr sorption was slightly higher than Co ($q^*_{mL,Co}/q^*_{mL,Sr} = 0.925$) in Co/Sr system. This result was conflicting with single-solute sorption where Co sorption was higher than Sr sorption onto IOCM ($q_{mL,Co}/q_{mL,Sr} = 1.068$). This is because the maximum sorption capacities of Co and Sr in both single- and bi-solute sorptions were similar. Among the $q^*_{mL,1}/q^*_{mL,2}$ ratios, the $q^*_{mL,Cs}/q^*_{mL,Sr}$ ratios were higher than 3 in all sorbents. This indicated that the Cs sorption was strongly superior to Sr sorption in Co/Sr system. All the q^*_{mL}/q_{mL} ratios were lower than unity (except Co of Cs/Co system in MOCM and IOCM), explaining that the sorption was hindered by the presence of the other competing metals. As the q^*_{mL}/q_{mL} ratio of a metal decreased, the sorption of such metal was more affected by the presence of the other competing metal. Especially, the $q^*_{mL,Cs}/q_{mL,Cs}$ ratios of montmorillonite in Cs/Co and Cs/Sr systems were lower than 0.39 which is the lowest in bi-solute competitive systems. The results indicated that Cs sorption can be heavily influenced by presence of high cation concentrations of other metals as previously reported by Galamboš et al. [33].

The bonding energy coefficient (b_L) for single-solute sorption and b^*_L for bi-solute competitive sorption) varied with sorbent type and relative affinity of the metal compared to competitive metals. As shown in Table 7, the $b^*_{L,Co}/b^*_{L,Sr}$ ratios in all sorbents were higher than unity indicating that Co sorbed more strongly onto the specific sorption sites than Sr in Co/Sr system. Whereas, the $b^*_{L,Cs}/b^*_{L,Sr}$ ratios in all sorbents were lower than unity indicating that Cs had weak sorption affinity than Sr onto the specific sorption sites in Cs/Sr system although $q^*_{mL,Cs}/q^*_{mL,Sr}$ ratios was higher than unity. In Cs/Co system, $b^*_{L,Cs}/b^*_{L,Co}$ ratios showed different tendency for different sorbents. The ratio was higher than unity in montmorillonite, but lower than unity in MOCM and IOCM. The sorption affinity of Cs was lower than that of Co due to both competition with Co and surface modification. The effect of metal competition on sorption

Table 7 Comparison of q_{mL} and b_L values of single-solute and bi-solute competitive sorption of Co, Sr and Cs at pH 6.0

Sorbent	Binary system (1)/(2)	$q_{mL,1}/q_{mL,2}$	$q^*_{mL,1}/q^*_{mL,2}$	$q^*_{mL,1}/q_{mL,1}$	$q^*_{mL,2}/q^*_{mL,2}$
Montmorillonite	Co/Sr	1.4117	2.0294	0.5275	0.6576
	Cs/Sr	5.7457	4.6400	0.3914	0.4847
	Cs/Co	4.0701	1.7637	0.3578	0.8258
MOCM	Co/Sr	1.3217	1.0646	0.6867	0.8524
	Cs/Sr	2.4248	3.5794	0.6213	0.4209
	Cs/Co	1.8346	1.8402	0.7986	1.0858
IOCM	Co/Sr	1.0680	0.9254	0.8493	0.9802
	Cs/Sr	2.9108	3.8647	0.8014	0.6035
	Cs/Co	2.7256	2.5258	0.9377	1.0119
Sorbent	Binary system (1)/(2)	$b_{L,1}/b_{L,2}$	$b^*_{L,1}/b^*_{L,2}$	$b^*_{L,1}/b_{L,1}$	$b^*_{L,2}/b_{L,2}$
Montmorillonite	Co/Sr	1.5601	1.3248	1.3196	0.9563
	Cs/Sr	0.2407	0.1077	3.0374	6.7511
	Cs/Co	0.1543	2.6427	3.0814	0.6041
MOCM	Co/Sr	1.4382	3.4465	0.7982	0.3331
	Cs/Sr	0.4339	0.1772	1.9738	4.8337
	Cs/Co	0.3017	0.4715	0.8507	0.5443
IOCM	Co/Sr	1.2372	2.3117	0.4920	0.2633
	Cs/Sr	0.2621	0.2525	1.7449	1.8106
	Cs/Co	0.2118	0.3213	0.7279	0.4937

q_{mL} and b_L values indicate Langmuir model parameters for single-solute sorption. q^*_{mL} and b^*_L indicate Langmuir model parameters for bi-solute competitive sorption. The metals in bi-solute competitive systems were labeled in the order of (1) and (2)

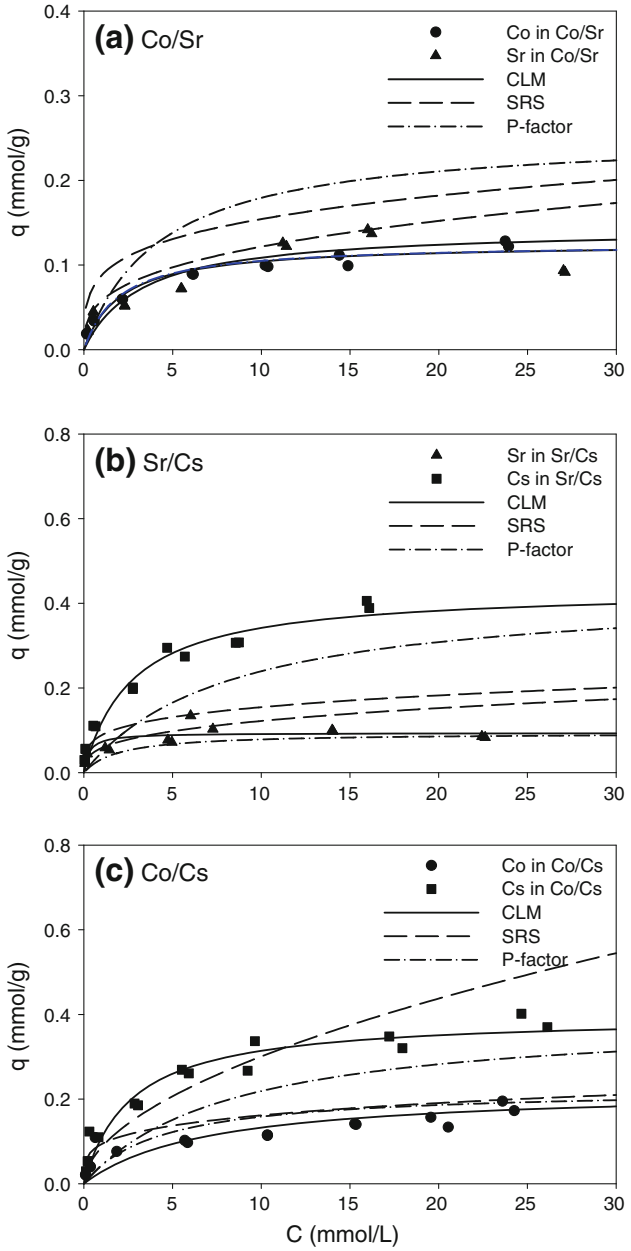

Fig. 8 Bi-solute competitive sorption of Co, Sr and Cs onto montmorillonite. *Lines* represent competitive sorption models

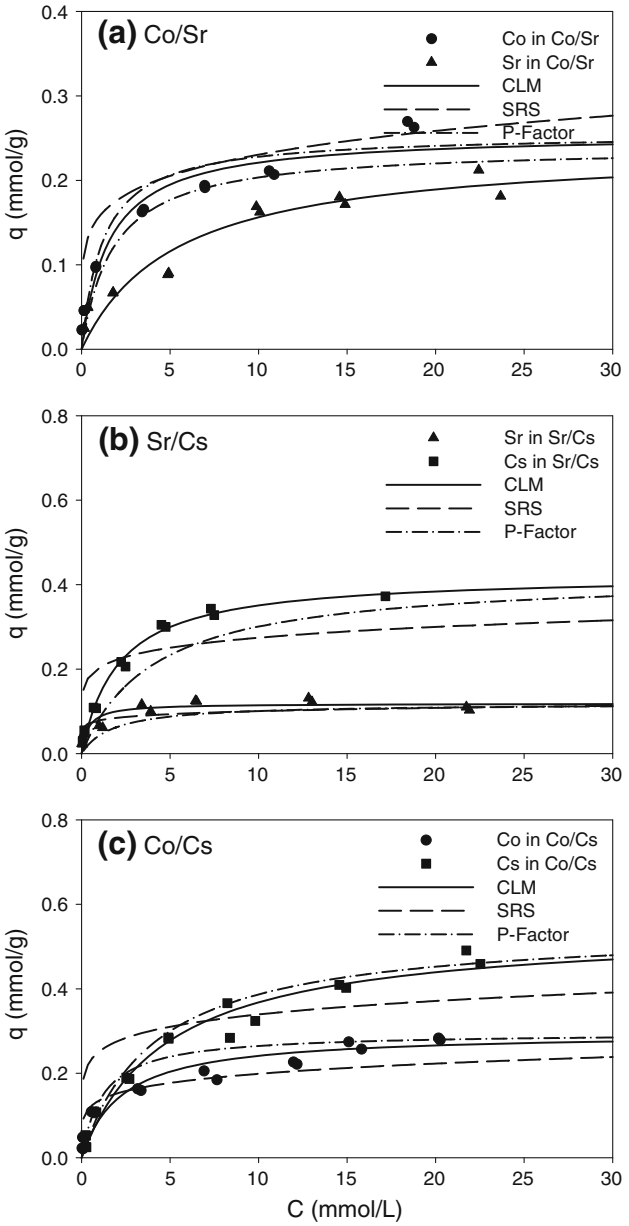

Fig. 9 Bi-solute competitive sorption of Co, Sr and Cs onto MOCM. *Lines* represent competitive sorption models

affinity in single-solute and bi-solute sorptions could be evaluated through the b^*_L/b_L ratios. In Cs/Sr system, both the $b^*_{L,Cs}/b_{L,Cs}$ and $b^*_{L,Sr}/b_{L,Sr}$ ratios were higher than unity regardless of the sorbent type. This indicated that the Cs or Sr sorption in Cs/Sr system had more sorption affinity than that in single-solute system. However, the b^*_L/b_L ratios in Co/Sr and Cs/Co systems were complicated. In Co/Sr and Cs/Co sorptions onto MOCM and ICOM, the b^*_L/b_L ratios were lower than unity indicating that the competition onto the sorption site reduced the sorption affinity of each metal compared to single-solute sorption. In montmorillonite, $b^*_{L,Co}/b_{L,Co}$ ratio in Co/Sr and $b^*_{L,Cs}/b_{L,Cs}$ ratio in Cs/Co were higher than unity, but, $b^*_{L,Sr}/b_{L,Sr}$ ratio in Co/Sr and $b^*_{L,Co}/b_{L,Co}$ ratio in Cs/Co were lower than unity.

Sheindorf-Rebhun-Sheintuch (SRS) model, competitive Langmuir model (CLM) and P-factor model (Figs. 8, 9, 10; Tables 8, 9, 10) were also applied to explain the bi-solute competitive sorptions of Co/Sr, Sr/Cs and Co/Cs onto the sorbents. The coefficient of determination (R^2), the sum of

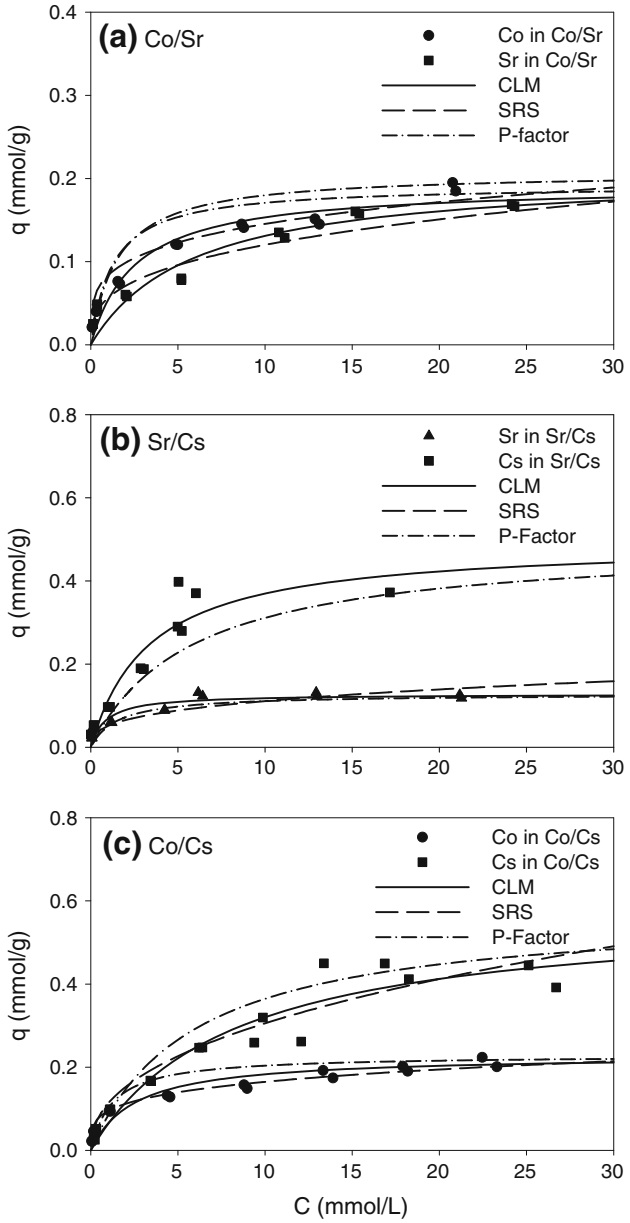

Fig. 10 Bi-solute competitive sorption of Co, Sr and Cs onto IOCM. *Lines* represent competitive sorption models

squared error (SSE) and the root mean square error (RMSE) were calculated by Eqs. 10, 11 and 12.

$$R^2 = \frac{\sum q_{i,\mathrm{exp}}^2 - \mathrm{SSE}}{\sum q_{i,\mathrm{exp}}^2} \tag{10}$$

$$\mathrm{SSE} = \sum_{i=1}^{N} (q_{i,\mathrm{exp}} - q_{i,\mathrm{pred}})^2 \tag{11}$$

$$\mathrm{RMSE} = \sqrt{\frac{\mathrm{rss}}{N_\mathrm{d} - P}} \tag{12}$$

where $q_{i,\mathrm{exp}}$ and $q_{i,\mathrm{pred}}$ represent experimental data and theoretically predicted points, respectively, and rss is the residual sum of squares, N_d is the number of data points, and P is the number of parameters.

In Figs. 8, 9, and 10, the SRS model predictions were in good agreement with experimental data for montmorillonite only, but not for MOCM and IOCM. Especially, two cases in MOCM (Sr in Co/Sr) and IOCM (Cs in Sr/Cs) were not successful. As summarized in Table 8, the competition coefficients, $\alpha_{i,j}$, of the SRS model explained the suppression of metal sorption due to competition. In all competitive systems, the α values were lower than 1, indicating that the metals affected each other in competitive sorption. In Sr/Cs sorption onto MOCM, Sr sorption ($\alpha_{12} > 3$) was more affected than Cs by competition, whereas Cs sorption was less affected ($\alpha_{21} < 1$). In Co/Cs sorption onto IOCM, both Co and Cs sorptions hardly affected each other ($\alpha_{12} < 0.1$ and $\alpha_{21} < 0.1$). Although the high R^2 values and low SSE and RMSE values indicated this model fitted well the experimental data, the SRS model predictions were less successful than CLM predictions.

The estimations of CLM were also fitted to the bi-solute competitive sorptions (Figs. 8, 9, and 10). As shown in Table 9, the CLM predicted the competitive sorptions successfully ($R^2 > 0.81$).

The P-factor model predictions were also presented in Figs. 8, 9, and 10 and the P-factor model parameters were listed in Table 10. Although P-factor model predictions

Table 8 SRS model parameters for bi-solute competitive sorption of Co, Sr and Cs

Sorbent	Solute	α_{12}	α_{21}	R^2	SSE	RMSE
Montmorillonite	Co/Sr	0.3164	0.1194	0.9288/0.9453	0.0033/0.0021	0.0527/0.0363
	Sr/Cs	0.1822	0.1534	0.8526/0.7425	0.0031/0.0601	0.0337/0.0622
	Co/Cs	0.2005	0.8054	0.9712/0.9107	0.0028/0.0408	0.0543/0.0643
MOCM	Co/Sr	0.5788	–	0.9528/–	0.0046/–	0.0413/–
	Sr/Cs	3.6983	0.9548	0.7539/0.0032	0.0044/0.1758	0.0215/0.0832
	Co/Cs	0.8777	0.5396	0.9569/0.0964	0.0063/0.3582	0.0671/0.1183
IOCM	Co/Sr	0.1415	0.2916	0.9288/0.9482	0.0033/0.0020	0.0152/0.0143
	Sr/Cs	0.4226	–	0.8272/–	0.0037/–	0.0192/–
	Co/Cs	0.0379	0.0338	0.9651/0.9274	0.0034/0.0331	0.0164/0.0449

Table 9 R^2 and SSE values for bi-solute competitive sorption predictions from competitive Langmuir model (CLM)

Sorbent	Solute	R^2	SSE	RMSE
Montmorillonite	Co/Sr	0.9862/0.9489	0.0006/0.0028	0.0116/0.0235
	Sr/Cs	0.9545/0.9862	0.0019/0.0054	0.0195/0.0327
	Co/Cs	0.9575/0.9602	0.0076/0.0290	0.0296/0.0643
MOCM	Co/Sr	0.9879/0.8099	0.0023/0.0109	0.0214/0.0462
	Sr/Cs	0.9748/0.9953	0.0015/0.0019	0.0176/0.0195
	Co/Cs	0.9780/0.9816	0.0103/0.0128	0.0354/0.0425
IOCM	Sr/Cs	0.9686/0.9245	0.0019/0.0244	0.0196/0.0691
	Co/Sr	0.9878/0.9731	0.0012/0.0023	0.0156/0.0212
	Co/Cs	0.9841/0.9616	0.0043/0.0266	0.0233/0.0558

Table 10 P-factor model parameters for bi-solute competitive sorption of Co, Sr and Cs

Sorbent	Solute	P_i	R^2	SSE	RMSE
Montmorillonite	Co/Sr	1.0678/1.5350	0.4276/0.9486	0.0569/0.0055	0.0719/0.0224
	Sr/Cs	2.0630/2.5547	0.8847/0.8697	0.0097/0.1015	0.0298/0.0961
	Co/Cs	1.2110/2.7947	0.9457/0.8976	0.0208/0.0975	0.0350/0.0866
MOCM	Co/Sr	1.4563/1.1731	0.9830/0.8738	0.0065/0.0285	0.0243/0.0509
	Sr/Cs	2.3758/1.6095	0.9223/0.9475	0.0350/0.0095	0.0295/0.0624
	Co/Cs	1.2561/1.2522	0.9752/0.9879	0.0221/0.0165	0.0361/0.0343
IOCM	Co/Sr	1.1774/1.0202	0.9624/0.8286	0.0076/0.0287	0.0263/0.0511
	Sr/Cs	0.9882/1.0664	0.9592/0.9190	0.0050/0.0563	0.213/0.0750
	Co/Cs	1.6568/1.2478	0.9731/0.9688	0.0148/0.0497	0.0295/0.0557

were in good agreement with the experimental data ($R^2 > 0.82$) except Co/Sr in montmorillonite ($R^2 = 0.43$), the P-factor model predictions were less satisfactory than CLM predictions. This is because this model is based on the Langmuir model and it does not consider the interactions and competitions that can influence the sorption capacity, thus, some deviations of the predicted curves from the experimental data are observed [24].

Conclusions

Single- and bi-solute competitive sorptions of Co, Sr and Cs ions onto the three different sorbents were investigated. The montmorillonite modified with Mn or Fe oxides showed high sorption capacity of Co and Sr than the pristine montmorillonite. This is due to increase in the CEC, reinforcing the negative charge in the surface and formation of possible sorption (adsorption and ion exchange) site for Co and Sr in the metal oxide-coated montmorillonite. However, the sorption capacity of Cs onto the metal oxide-coated montmorillonite was lower than those onto pristine montmorillonite. This is because the sorption site for Cs on the pristine montmorillonite was covered with coated metal oxide and thus Cs sorbed only onto more preferable site on the metal oxide-coated montmorilonite. In bi-solute competitive sorptions, the maximum sorption capacity of one metal decreased due to the presence of competing metal ion. Mn and Fe oxides easily combined with clay materials in nature. By artificially coating the pristine montmorillonite with Mn oxides, sorption site in the clay could be more vitalized. Hence, the Mn oxide-coated montmorillonite become more applicable to remove Co and Sr in groundwater. However, Fe oxide coating onto the surface of montmorillonite improved Sr sorption capacity but not Co and Cs. The pristine montmorillonite and the metal oxide-coated montmorillonites are environmentally friendly sorbents which are not harmful to groundwater system and thus they can be used for the removal of Co, Sr and Cs.

Acknowledgments This research was supported by Korea Science and Engineering Foundation (KOSEF) grant funded by the Korean government, the Ministry of Education, Science and Technology (grant number: M20709005401-07B0900-40110) and the authors acknowledge the Korea Basic Science Institute (Daegu) and Kyungpook National University Center for Scientific Instrument.

References

1. Ragnarsdottir KV, Fournier P, Oelkers EH, Harrichoury JC (2001) Geochim Cosmochim Acta 65:3955–3964

2. Abalkina IL, Sarkisov AA, Linge II, Kazakov SV, Panchenko SV, Savelieva EA (2008) Appl Radiat Isot 66:1554–1557
3. El-Kamash AM (2008) J Hazard Mater 151:432–445
4. Bowyer TW, Biegalski SR, Cooper M, Eslinger PW, Haas D, Hayes JC, Miley HS, Strom DJ (2011) J Environ Radioact 102:681–687
5. World Health Organization (2006) WHO, Gevana, Switzerland
6. Yoon YY, Cho SY, Lee KY, Kim Y (2006) J Korean Assoc Radiat Prot 31:25–30
7. Conca JL, Wright J (2006) Appl Geochem 21:1288–1300
8. Noubactep C (2006) J Radioanal Nucl Chem 267:13–19
9. Noubactep C, Schöner A, Dienemann H, Sauter M (2006) J Radioanal Nucl Chem 267:21–27
10. Riebe B, Dultz S, Bunnenberg C (2005) Appl Clay Sci 28:9–16
11. Karamanis DT, Aslanoglou XA, Assimakopoulos PA, Gangas NH (1999) J Radioanal Nucl Chem 242:3–9
12. Al-Degs Y, Khraisheh MAM, Tutunji MF (2001) Water Res 35:3724–3728
13. Oliveria LCA, Rios RVRA, Fabris JD, Sapag K, Garg VK, Lago RM (2003) Appl Clay Sci 22:169–177
14. Vicente MA, Lambert JF (2010) Phys Chem Chem Phys 3:4843–4852
15. Simon FG, Segebade C, Hedrich M (2003) Sci Total Environ 207:231–238
16. Versada J, Hradil D, Řanda Z, Jelínek E, Štulík K (2005) Appl Clay Sci 30:53–66
17. Khraisheh MAM, Al-degs YS, Mcminn WAM (2004) Chem Eng J 99:177–184
18. USEPA (2003) US EPA Method 9081, SW-846, Office of Solid Waste. Washington, DC
19. Ma B, Oh S, Shin WS, Choi SJ (2011) Desalination 276:336–346
20. Wolff-Boenisch D, Traina SJ (2006) Geochim Cosmochim Acta 70:4356–4366
21. Kundu S, Gupta AK (2006) Chem Eng J 122:93–106
22. Sheindorf C, Rebhun M, Sheintuch M (1881) J Colloid Interf Sci 79:136–142
23. Srivastava VC, Mall ID, Mishra IM (2006) Chem Eng J 117:79–91
24. Valderrama C, Barios JI, Rarran A, Cortina JL (2010) Water Air Soil Pollut 210:421–434
25. Choy KKH, Proter JF, Mckay G (2000) J Chem Eng Data 45:575–584
26. Yu S, Ren A, Cheng J, Song XP, Chen C, Wang X (2007) J Radioanal Nucl Chem 273:129–133
27. Boonfueng T, Axe L, Xu T (2005) J Colloid Interf Sci 281:80–92
28. Ijagbemi CO, Baek MH, Kim DS (2009) J Hazard Mater 166:538–546
29. Nachtegaal M, Sparks DL (2004) J Colloid Interf Sci 276:13–23
30. Changtawong V, Harvey NW, Bashkin VN (2003) Water Air Soil Pollut 148:111–125
31. Bhattacharyya KG, Gupta SS (2007) J Colloid Interf Sci 310:411–424
32. Wen T, Chen Y, Cai L (2011) J Radioanal Nucl Chem 290:437–446
33. Galamboš M, Paučová V, Kufčáková J, Rosskopfová O, Rajec P, Adamcová R (2010) J Radioanal Nucl Chem 284:55–64
34. Ararem A, Bouras O, Arbaoui F (2011) Chem Eng J 172:230–236
35. McKay G, Blair HS, Gardner JR (1982) J Appl Polym Sci 27:3040–3057
36. Başçetin E, Atun G (2006) Appl Radiat Isot 64:957–964
37. Zhang SQ, Hou WG (2008) Colloid Surface A: Physicochem Eng Aspects 320:92–97
38. Bhattacharyya KG, Gupta SS (2008) Adv Colloid Interf Sci 140:114–131
39. Kanungo SB, Tripathy SS, Rajeev (2004) J Colloid Interf Sci 269:1–10
40. Gutierrez M, Ruentes HR (1996) Appl Clay Sci 11:11–24
41. Chirkst DE, Cheremisina OV, Ivanov MV, Chistyakov AA, Zhadovskii IT (2006) Russian J Appl Chem 79:367–371
42. Nightingale ER (1959) J Phys Chem 63:1381–1387
43. Wu J, Li B, Liao J, Feng Y, Zhang D, Zhao J, Wen W, Yang Y, Liu N (2009) J Environ Radioact 100:914–920
44. Iijima K, Tomura T, Shoji Y (2010) Appl Clay Sci 49:262–268